An improved strategy to detect CO_2 leakage for verification of geologic carbon sequestration

J. L. Lewicki,[1] G. E. Hilley,[2] and C. M. Oldenburg[1]

Received 2 August 2005; revised 26 August 2005; accepted 14 September 2005; published 15 October 2005.

[1] The long-term storage of CO_2 must be verified to ensure the success of geologic carbon sequestration projects. To detect subtle CO_2 leakage signals, we present a strategy that integrates near-surface measurements of CO_2 fluxes or concentrations with an algorithm that enhances temporally- and spatially-correlated leakage signals while suppressing random background noise. We assess the performance of this strategy using synthetic CO_2 flux data sets and modeled surface CO_2 leakage. These simulations provide a means of estimating the number of measurements required to detect a potential CO_2 leakage signal of given magnitude and area. Results show that given a rigorous and well-planned field sampling program, subtle surface CO_2 leakage may be detected using the algorithm; however, leakage of very limited spatial extent or exceedingly small magnitude may be difficult to detect with a reasonable set of monitoring resources. **Citation:** Lewicki, J. L., G. E. Hilley, and C. M. Oldenburg (2005), An improved strategy to detect CO_2 leakage for verification of geologic carbon sequestration, *Geophys. Res. Lett.*, *32*, L19403, doi:10.1029/2005GL024281.

1. Introduction

[2] One strategy to mitigate potential climate change associated with elevated atmospheric CO_2 concentrations is the sequestration of anthropogenic CO_2 in deep geologic formations [e.g., *International Energy Agency*, 1997; *Reichle et al.*, 1999]. While the purpose of geologic carbon sequestration is to trap CO_2 underground, the potential exists for CO_2 to leak from the storage site along permeable pathways such as well bores or faults and pass from the subsurface to the atmosphere. Although surface CO_2 leakage fluxes may be small, they could represent a significant loss of CO_2 over the several-hundred-year time scales required for CO_2 storage to be effective against climate change [*Hepple and Benson*, 2002], and cause adverse health, safety, and environmental effects.

[3] Due to the potentially negative effects of CO_2 leakage, it is important that storage verification be conducted as an integral part of geologic carbon sequestration. Although numerous technologies are available to measure near-surface CO_2, storage verification may be challenging due to the large variation in natural background CO_2 fluxes and concentrations [e.g., *Buyanovsky and Wagner*, 1983; *Osozawa and Hasegawa*, 1995; *Xu and Qi*, 2001; *Lewicki et al.*, 2003], within which a potentially small CO_2 anomaly may be hidden.

[4] We present a strategy that integrates near-surface measurements of CO_2 with statistical analysis to enhance properties of the data that are associated with leakage, while reducing random background contributions. Using a suite of synthetic CO_2 flux data sets and modeled CO_2 surface leakage from a flow and transport simulator, we investigate various combinations of sampling and analysis approaches to optimize leakage detection and quantification while minimizing the number of measurements. We discuss implications for geologic carbon storage verification and other studies where detection of a small anomalous signal within background noise is required.

2. Methods

[5] Our filtering method exploits several contrasting properties of near-surface CO_2 fluxes and concentrations derived from natural background processes versus those from CO_2 leakage. First, the production of CO_2 by background processes (e.g., soil respiration) is highly spatially heterogeneous; resulting soil CO_2 fluxes and concentrations are therefore poorly correlated on moderate to large spatial scales (e.g., $\geq$5 m) [e.g., *Stoyan et al.*, 2000; *Xu and Qi*, 2001; *Lewicki et al.*, 2003]. In contrast, CO_2 derived from leakage along e.g., a well bore or fault, should be relatively coherent in space. Second, the production of background CO_2 is controlled by meteorological and biological processes operating on diurnal to seasonal time scales and is therefore correlated on these time scales [e.g., *Buyanovsky and Wagner*, 1983; *Osozawa and Hasegawa*, 1995; *Ouyang and Zheng*, 2000; *Xu and Qi*, 2001; *Tang et al.*, 2003]. In contrast, the leakage of CO_2 from a storage reservoir should be relatively constant. Finally, near-surface CO_2 from both background sources and leakage will be modified by meteorological and biological processes on predictable time scales. Temporal variations in measured soil CO_2 fluxes and concentrations related to these background processes can be removed at predictable wavelengths [*Lewicki et al.*, 2003]. Thus, if one measures soil CO_2 fluxes/concentrations in an area in which there may be a small CO_2 leakage signal within background variability, this data can be adjusted to eliminate temporal variability associated with background processes. Areas of elevated spatial and temporal correlation in CO_2 associated with leakage can then be made more obvious.

[6] The algorithm used to detect and quantify leakage consists of a filter that highlights spatial coherence, and temporal averaging that reduces noise from temporally uncorrelated background fluxes. To highlight spatial coherence, we progressively move a Gaussian weighting function

[1]Earth Sciences Division, Lawrence Berkeley National Laboratory, Berkeley, California, USA.
[2]Department of Geological and Environmental Sciences, Stanford University, Stanford, California, USA.

0094-8276/05/2005GL024281$05.00

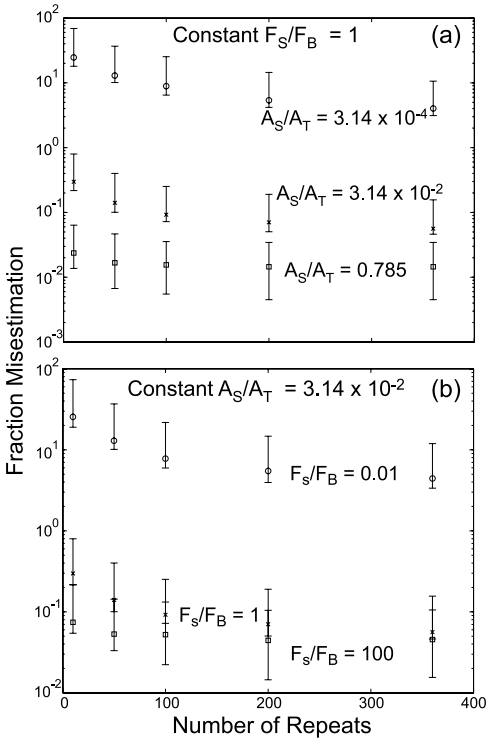

Figure 1. Fraction misestimation (f_{ME}) versus number of repeat sampling campaigns for (a) $A_S/A_T = 3.14 \times 10^{-4}$ (circles), 3.14×10^{-2} (x's), and 0.785 (squares) and constant F_S/F_B (= 1) and (b) $F_S/F_B = 0.01$ (circles), 1 (x's), and 100 (squares) and constant A_S/A_T (= 3.14×10^{-2}).

over a regularly spaced (5 m) grid, and use this function to calculate the weighted average of all measured points according to their distance from the specified grid point. To reduce temporally uncorrelated noise, we either (1) average repeated measurements at each sampling location, then apply the Gaussian weighting function, or (2) average flux values at each grid point interpolated using the Gaussian weighting function based on repeated measurements at each sample location.

[7] To test different sampling and processing combinations, we created a suite of synthetic data sets in which surface CO_2 leakage was treated as a two-dimensional scaled Gaussian distribution. To simulate CO_2 signals associated with leakage along a well bore and a fault, we used the simulator T2CA [*Oldenburg and Unger*, 2003], a research module of TOUGH2 [*Pruess et al.*, 1999] (see Supplement 1[1] for properties of the model system). In both cases, background biological noise was added to the surface CO_2 leakage and surrounding area (10^6 m^2) using a log-normal CO_2 flux distribution measured using the accumulation chamber method [e.g., *Norman et al.*, 1992] at 287 locations in grassland in central California and uncorrelated on spatial scales $\geq$5 m [*Lewicki et al.*, 2003]. These data were adjusted to remove diurnal fluctuations and then the mean, F_B, and standard deviation were calculated (=8.7 and 6.7 g $m^{-2}d^{-1}$, respectively). Thus, modeled background fluxes represent the case in which temporal correlation has been removed. To model re-measurement of fluxes over time, a new realization of the background synthetic data set was repeatedly drawn from the distribution and superimposed on the leakage.

[8] Using a suite of these synthetic data sets, we explored a range of sampling and processing strategies. In each, we sampled 100 CO_2 fluxes from the underlying synthetic data set. The following strategies were explored: (1) CO_2 fluxes were sampled on a regularly-spaced grid on multiple campaigns, Gaussian filtering was applied to each data set, and fluxes at each interpolated grid point were temporally averaged; (2) fluxes were randomly sampled in space, sampling was repeated at the same locations over time, Gaussian filtering was applied to each data set, and fluxes at each interpolated grid point were temporally averaged; (3) fluxes were randomly sampled in space and were re-randomized during each re-sampling, Gaussian filtering was applied to each data set, and fluxes at each interpolated grid point were temporally averaged. Then, strategies (1) and (2) were repeated, where the order of the filtering and stacking procedures was reversed. Strategy success was judged based on the fraction misestimation (f_{ME}) of the total CO_2 leakage rate ($=\sqrt{(\textit{Imposed Leakage Rate} - \textit{Calculated Leakage Rate})^2}/\textit{Imposed Leakage Rate}$), where the leakage rate is the spatially integrated leakage flux of the synthetic source.

3. Results

[9] Strategy (3) most consistently detected surface CO_2 leakage of arbitrary magnitude, area, and location. Supplement 2 shows an example of this strategy. A CO_2 leakage flux signal of known magnitude and dimension (maximum leakage CO_2 flux, F_S = 1.7 g m^{-2} d^{-1}; Gaussian length scale, R = 100 m) was imposed at x = 250 m, y = 250 m (Supplement 2a). Next, time-adjusted background noise was superimposed on this signal (Supplement 2b shows one realization of the underlying synthetic data set in time). From this synthetic data set, 100 CO_2 fluxes were randomly sampled (Supplement 2c), and the process shown in Supplement 2b and c was repeated 100 times to represent repeated sampling campaigns, re-randomizing the sample locations each time. The Gaussian filter was applied to each of the 100 flux sample sets, and then point-by-point temporal averaging was applied. The final result (Supplement 2d) shows that this method identifies the CO_2 leakage location, although the peak flux magnitudes are underestimated, and the spatial extent of the signal is overestimated due to Gaussian filtering. The total CO_2 leakage rate of the synthetic source agrees well with that recovered by the algorithm, with f_{ME} = 0.02.

[10] We varied the number of repeat sampling campaigns (=10, 50, 100, 200, and 360) for R/L = 0.01, 0.1, and 0.5 (L = model domain length in x and y directions = 1000 m), while holding F_S/F_B constant (=1) (Figure 1a). These R/L values correspond to ratios of the synthetic leakage signal area (A_S) to the total area of the model domain ($A_T = 10^6$ m^2) of 3.14×10^{-4}, 3.14×10^{-2}, and 0.785. To estimate the distribution of f_{ME} for each case, we performed 100 Monte Carlo realizations of each number of sampling campaigns. The mean and 68% lower and upper bounds of f_{ME} are plotted in Figures 1 and 2. We then varied the number of

[1]Auxiliary material is available at ftp://ftp.agu.org/apend/gl/2005GL024281.

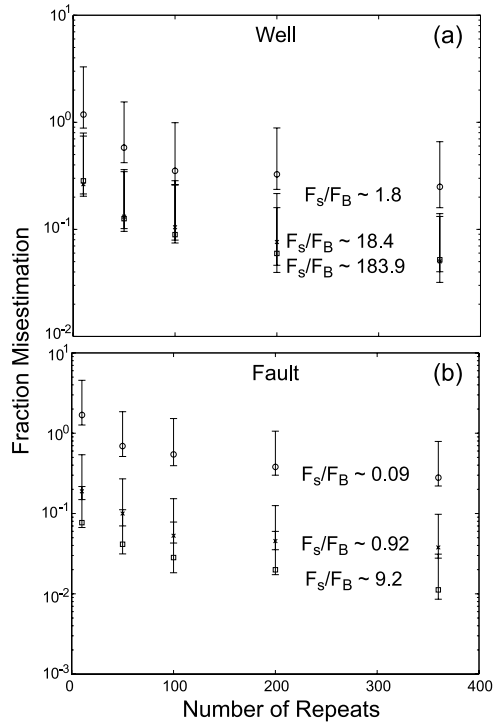

Figure 2. Fraction misestimation (f_{ME}) versus number of repeat sampling campaigns for (a) well scenarios where $F_S/F_B \sim 1.8$ (circles), 18.4 (x's), and 184.9 (squares) and $A_S/A_T \sim 4.34 \times 10^{-2}$ and (b) fault scenarios where $F_S/F_B \sim 0.09$ (circles), 0.92 (x's), and 9.2 (squares) and $A_S/A_T \sim 0.161$.

sampling campaigns for F_S/F_B = 0.01, 1, and 100, while holding A_S/A_T constant (=3.14×10^{-2}) (Figure 1b). Figures 1a and 1b show that for a given A_S/A_T or F_S/F_B, f_{ME} decreases non-linearly as the number of sampling campaigns increases, with f_{ME} becoming relatively insensitive to number of sampling campaigns >100. Also, f_{ME} is insensitive to the number of sampling campaigns at the highest A_S/A_T or F_S/F_B values considered relative to lower values. For a given number of sampling campaigns, f_{ME} decreases with A_S/A_T or F_S/F_B by up to ~2.5 orders of magnitude. However, f_{ME} becomes less sensitive to A_S/A_T or F_S/F_B as A_S/A_T or F_S/F_B increases. Regardless of the number of sampling campaigns, f_{ME} is highest at the lowest A_S/A_T or F_S/F_B values and lowest at the highest A_S/A_T or F_S/F_B values.

[11] To consider more physically realistic cases, we modeled two leakage scenarios. First, an abandoned well that is open at depth, but plugged in the near-surface transports CO_2 from a deep storage reservoir to the vadose zone. In the other, a buried fault transports CO_2 to the vadose zone. A CO_2 source was specified in either the fault (linear, 10 × 1000 m) or well (point, 1 × 1 m) geometry at an arbitrary depth of −27.1 m in a three-dimensional vadose zone (Supplement 1) with surface area = 10^6 m^2. Because we presently do not know the magnitude of leakage fluxes expected from a storage reservoir, the low, medium, and high source leakage fluxes for the well (3.8×10^4, 3.8×10^5, and 3.8×10^6 g m^{-2}d^{-1}, respectively) and fault (3.8, 38, and 380 g m^{-2}d^{-1}, respectively) scenarios were chosen to generate F_S values over a range of CO_2 fluxes observed in nature, from relatively low-flux biological environments to high-flux volcanic environments [e.g., *Chiodini et al.*, 1998; *Lewicki et al.*, 2005], and assess a range of f_{ME} values for the two scenarios (i.e., test the limits of the method). The surface leakage fluxes we consider (Supplement 3) result from upward and lateral CO_2 advection, diffusion, and interaction with vadose zone pore water and are calculated at t = 100 y of model time, at which time they are nearly steady. F_S values corresponding to low, medium, and high leakage fluxes for well simulations are ~16, 160, and 1600 g m^{-2}d^{-1} (F_S/F_B ~1.8, 18.4, 183.9), and for fault simulations are ~0.8, 8, and 80 g m^{-2}d^{-1} (F_S/F_B ~0.09, 0.92, 9.2).

[12] Figure 2 shows that for a given F_S/F_B for both well and fault scenarios, f_{ME} decreases non-linearly with increasing number of sampling campaigns, to become relatively constant at >200 repeats. However, even though the low, medium, and high F_S/F_B cases for the fault scenario are ~two orders of magnitude lower than those for the well scenario, f_{ME} values are similar. For a given number of sampling campaigns, f_{ME} decreases with increasing F_S/F_B.

4. Discussion and Conclusions

[13] For a given number of sampling campaigns, f_{ME} is sensitive to both F_S/F_B and A_S/A_T. If we conservatively assume that f_{ME} values ≤0.5 represent leakage anomalies detectable within a reasonable error and values >0.5 are "undetectable" anomalies, we can make the following statements. (1) Leakage with $A_S/A_T \geq 3.14 \times 10^{-2}$ and F_S/F_B = 1 is detectable with only 10 sampling campaigns; that with $A_S/A_T = 3.14 \times 10^{-4}$ is undetectable with up to 360 campaigns (Figure 1a). (2) Leakage with $F_S/F_B \geq 1$ and $A_S/A_T = 3.14 \times 10^{-2}$ is detectable with only 10 sampling campaigns; that with F_S/F_B = 0.01 is undetectable with up to 360 campaigns (Figure 1b). (3) Simulated surface leakage resulting from CO_2 leakage from an abandoned well with A_S/A_T ~4.34×10^{-2} and $F_S/F_B \geq 18.4$ is detectable with only 10 sampling campaigns; that with F_S/F_B = 1.8 requires at least 100 repeats (Figure 2a). (4) Simulated surface leakage resulting from CO_2 leakage from a buried fault with A_S/A_T ~0.161 and $F_S/F_B \geq 0.92$ is detectable with only 10 sampling campaigns; that with F_S/F_B = 0.09 requires at least 200 repeats (Figure 2b).

[14] Due to the relatively high A_S/A_T of simulated leakage anomalies associated with the fault source, it is possible to detect anomalies with low F_S (i.e., $\leq F_B$) with a reasonable (see below) number of samples. This emphasizes the importance of maximizing A_S/A_T in studies where seepage fluxes could have F_S within the background variability of CO_2 flux or could have small A_S (e.g., wells, mostly sealed faults/fractures). While we explored a large, reservoir-scale area, A_S/A_T could be maximized by reducing A_T, thereby increasing ability to detect leakage anomalies with fewer sampling campaigns. For example, the locations of potential conduits for fluid transport should be located and sampling should be focused within these smaller areas. Additionally, potential diffuse leakage through storage reservoir caprock over a large area would result in high A_S/A_T and should be detectable with relatively few samples.

[15] We based our example on soil CO_2 flux measurements made using the accumulation chamber method due to its well-tested reliability, the rapidity of each measurement (typically a few minutes), and the availability of a large

background CO_2 flux data set collected using this method. However, our strategy could equally apply to other gas species, to subsurface gas concentrations measured using a portable gas analyzer, and potentially to gas concentrations in surface water. Due to our ability to rapidly measure soil CO_2 flux or concentration over variable terrain conditions, making 100 measurements within a study area within a given day is reasonable in most circumstances. Hence, the number of repeat sampling campaigns will equal the number of days required to devote to storage verification. In most cases, 10–50 repeat sampling campaigns should be reasonable within a year; a greater number will depend on available resources.

[16] Our analysis treats background CO_2 fluxes and concentrations as statistically uniform over a study area. This may not be the case if there are features (e.g., topography, vegetation) that cause relatively consistent CO_2 production over time. While background CO_2 signals in these areas could be misinterpreted as subtle leakage, careful analysis of properties of the study area in conjunction with soil gas chemical (e.g., CO_2 and O_2 concentration profiles with depth) and isotopic analyses should allow one to distinguish the two sources. Our analysis also assumes that CO_2 leakage is slowly evolving over the observation period. If there is interest to detect leakage that is rapidly changing, which may be the case in the early stages of CO_2 leakage into the near-surface or during mitigation efforts, then additional analysis taking into account a temporally evolving source will be required. In either case, our strategy provides a simple means to locate and quantify potentially small CO_2 leakage derived from geologic storage reservoirs within the natural background variability of CO_2. If leakage is detected, then further geophysical, geochemical, and reservoir management techniques can be applied to locate and mitigate the leak.

[17] **Acknowledgments.** This work was supported in part by a Cooperative Research and Development Agreement between BP Corporation North America, as part of the CO_2 Capture Project, and the U.S. Department of Energy through the National Energy Technologies Laboratory, and by the Ernest Lawrence Berkeley National Laboratory, managed for the U.S. Department of Energy under Contract No. DE-AC03-76SF00098. We thank G. Chiodini, D. Vasco, and an anonymous reviewer for constructive review of this manuscript.

References

Buyanovsky, G. A., and G. H. Wagner (1983), Annual cycles of carbon dioxide level in soil air, *Soil Sci. Soc. Am. J.*, *47*, 1139–1145.

Chiodini, G., G. R. Cioni, M. Guidi, B. Raco, and L. Marini (1998), Soil CO_2 flux measurements in volcanic and geothermal areas, *Appl. Geochem.*, *13*, 543–552.

Hepple, R., and S. M. Benson (2002), Implications of surface seepage on the effectiveness of geologic storage of carbon dioxide as a climate change mitigation strategy, in *Greenhouse Gas Control Technologies*, edited by J. Gale and Y. Kaya, pp. 261–266, Elsevier, New York.

International Energy Agency (1997), Carbon Dioxide Utilization, IEA Greenhouse Gas R and D Programme, Paris.

Lewicki, J. L., W. C. Evans, G. E. Hilley, M. L. Sorey, J. D. Rogie, and S. L. Brantley (2003), Shallow soil CO_2 flow along the San Andreas and Calaveras faults, CA, *J. Geophys. Res.*, *108*(B4), 2187, doi:10.1029/2002JB002141.

Lewicki, J. L., D. Bergfeld, C. Cardellini, G. Chiodini, D. Granieri, N. Varley, and C. Werner (2005), Comparative soil CO_2 flux measurements and geostatistical estimation methods on Masaya volcano, Nicaragua, Bull. Volcanol., doi:10.1007/s00445-005-0423-9, in press.

Norman, J. M., R. Garcia, and S. B. Verma (1992), Soil surface CO_2 fluxes and the carbon budget of a grassland, *J. Geophys. Res.*, *97*, 18,845–18,853.

Oldenburg, C. M., and J. A. Unger (2003), On leakage and seepage from geologic carbon sequestration sites: Unsaturated zone attenuation, *Vadose Zone J.*, *2*, 287–296.

Osozawa, S., and S. Hasegawa (1995), Diel and seasonal changes in carbon dioxide concentration and flux in an andisol, *Soil Sci.*, *160*, 117–124.

Ouyang, Y., and C. Zheng (2000), Surficial processes and CO_2 flux in soil ecosystem, *J. Hydrol.*, *234*, 54–70.

Pruess, K., C. Oldenburg, and G. Moridis (1999), TOUGH2 user's guide version 2.0, *Rep. LBNL-43134*, Lawrence Berkeley Natl. Lab., Berkeley, Calif.

Reichle, D., et al. (1999), Carbon sequestration research and development, *Rep. DOE/SC/FE-1*, U.S. Dep. of Energy, Washington, D. C.

Stoyan, H., H. De-Polli, S. Bohm, G. P. Robertson, and E. A. Paul (2000), Spatial heterogeneity of soil respiration and related properties at the plant scale, *Plant Soil*, *222*, 203–214.

Tang, J., D. D. Baldocchi, Y. Qi, and L. Xu (2003), Assessing soil CO_2 efflux using continuous measurements of CO_2 profiles in soils with small solid-state sensors, *Agric. For. Meteorol.*, *118*, 207–220.

Xu, M., and Y. Qi (2001), Soil-surface CO_2 efflux and its spatial and temporal variations in a young ponderosa pine plantation in northern California, *Global Change Biol.*, *74*, 667–677.

G. E. Hilley, Department of Geological and Environmental Sciences, 450 Serra Mall, Braun Hall, Building 320, Stanford University, Stanford, CA 94305-2115, USA.

J. L. Lewicki and C. M. Oldenburg, Earth Sciences Division, Lawrence Berkeley National Laboratory, 1 Cyclotron Road, MS 90-1116, Berkeley, CA 94720, USA. (jllewicki@lbl.gov)